Proceedings of the 17th World Congress
The International Federation of Automatic Control
Seoul, Korea, July 6-11, 2008

Model Identification Dedicated to the Time-Optimal Control

A. Turnau*

**AGH University of Science and Technology, Kraków, Poland (e-mail: atu@agh.edu.pl)*

Abstract: A model identification procedure is applied to the well known benchmark problem of the pendulum hinged to a cart. There is a dynamical model of the entire system. The PWM control signal and DC motor impact introduced electrically by EMF are included. A concatenation of trajectories collected during several control experiments is used to fit the parameters of the pendulum-cart mathematical model. The identification of model parameters is dedicated to the control goal. Several collected points of trajectories are neglected. The model matching corresponds to intervals.

1. INTRODUCTION

Models can come from introspection (based on laws of nature) or/and observation (behavioral models). The goal is to find a functional form (a model architecture) and determine its adjustable parameters to best describe a set of collected experimental data. In other words, to obtain the best matching between the predictions of the model and the data. In general, we deal with three sets: different model architectures a, model parameters c and measurement data d (Gershenfeld, 1999). The data are compound of measured signals and noise. Moreover, if stochastic effects are present the concept of a random variable x and its distribution $p(x)$ has to be introduced, where $\int_{\alpha}^{\beta} p(x)dx$ is probability to observe x between α and β. For a joint random variable according to Bayes' rule we can define the conditional probability. Therefore the Bayesian model estimation should result in finding c that are most likely given the choice of a and d. We have decided to stick with one model architecture a i.e., a model described by ODE (analytical state and conjugate equations). Nevertheless their complex form we can simply derive the conjugate equations with the help of symbolic methods (MAPLE). A set of N noisy measurements (a sample) $y_n = y(x_n, c)$ as a function of a variable x_n and coefficients c is given. All measurements are thus trajectory points collected in real-time from sensors for a given system. The errors of measurement data, $e_n = y_n - y$ are assumed to be normal (having a Gaussian distribution) because many random variables of practical interest are normal or approximately normal or easy transformed into normal random variables Errors between samples are independent and identically distributed i.e., the probability to see the entire data set is equal to the product of the probabilities to see each point (Eykhoff, 1974). Finally, we use the method of least squares: $\min_{c} \sum_{n=1}^{N} [y_n - y(x_n, c)]^2$.

We can assume $\sigma_n^2 = 1$ if the standard deviations σ_n^2 is not known in advance. The least squares formula is easily optimized if it can be expand as a linear sum of k known basis functions. These are not however our cases. We deal with much more general examples where the coefficients c are inside the nonlinear basis functions. Starting from guess for c the estimate is refined. Such a nonlinear optimization can be stopped at a local minimum. There is no guarantee that the local and global minima are the selfsame. However, for a small number of c parameters (six in our case) it is a numerical evidence – as it will be illustrated in section 3 – that the attained minimum can be recognized as the global one. We have to emphasis that the identified model corresponds to real system trajectories of a special type. These trajectories respond to "bang-bang" controls. Therefore they are only a subset of all possible trajectories. Moreover, to fit better to the "bang-bang" optimal controls and to neglect a no homogenous static friction we can delete the trajectory points for a motionless system or the points being at the beginning of motion. In this way we focused our identification procedure not only to the "bang-bang" control trajectories but also to a piece-wise parameter fitting – only intervals of the entire trajectory are taken into account (see Fig. 4 in section 3 that illustrates how the intervals are generated due to the small velocities zone). Such an approach was described in (Marchewka, et al., 2005) for the first time.

2. THE CART AND PENDULUM BENCHMARK

Consider the system depicted in Fig. 1.

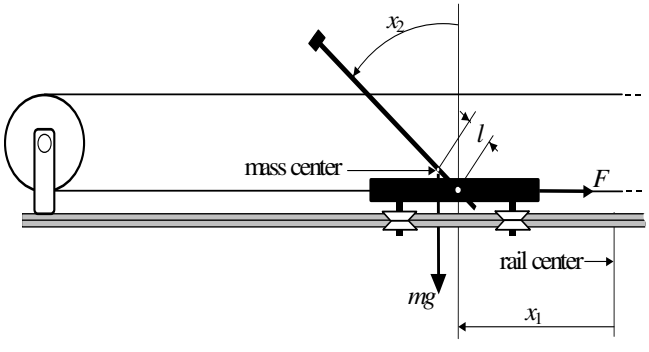

Fig. 1. Pendulum on a cart system

A pendulum rotates in a vertical plane around an axis located on a cart. The cart can move along a horizontal rail, lying in the plane of rotation. The cart is pulled forth and back by a DC motor via a belt drive encircling two belt pulleys. The state of the system is a vector $x = \mathrm{col}(x_1, x_2, x_3, x_4)$ where x_1 is the cart position, x_2 is the angle between the upward direction and the pendulum, measured counterclockwise ($x_2 = 0$ for the upright position of the pendulum), x_3 is the cart velocity, and x_4 is the pendulum angular velocity. The computer control $u(t)$ takes values in the interval $[-u_{\max}, u_{\max}]$, where $u_{\max}$ is the unit-less maximal magnitude of a pulse width modulation (PWM) signal generated by the I/O computer board. For simplicity, $u(t)$ is replaced by u. Consequently, the t parameter will be omitted in the formulas. The signal u multiplied by the voltage gain K_u becomes the input voltage to DC motor, $u \cdot K_u$. A control force F generated by a DC flat motor, parallel to the rail, is applied to the cart

$$F = p_1 u + p_2 x_3, \tag{1}$$

where p_1 and p_2 are respectively the control force to PWM signal and control force to cart velocity ratios

$$p_1 = \varepsilon K_u, \quad p_2 = -\varepsilon \frac{60}{2\pi \cdot 10^3} \frac{U_{rpm}}{r_d}, \tag{2}$$

where

$$\varepsilon = \frac{M_i}{r_d R_i}.$$

The total mass of the pendulum and cart is denoted by m. The armature circuit dynamics is neglected. That is justified due to a very small time constant. Of course, the motor has a big impact for the entire control system and it is present in the model: electrically by EMF the electro-magnetic force to rpm (rotation per minute) ratio i.e., U_{rpm} involved in p_2 and mechanically by an equivalent mass m_e (the total mass m has to be increased to involve inertial effects of the armature and belt pulleys). l is the distance from the axis of rotation of the pendulum to the center of mass of the system. J is the moment of inertia of the pendulum with respect to its rotational axis on the cart. The cart friction is compound of two forces: the static Coulomb friction, $\mathrm{sign}(x_3) F_s$ and the viscous friction proportional to the cart velocity, $f_c x_3$. The discontinuous "sign" function is approximated by $\tanh(n x_3)$ where n is an natural number i.e., $n = 10$. There is also a friction torque in the angular motion of the pendulum, proportional to the angular velocity, $f_p x_4$. M_i and R_i are parameters of the DC motor and denote respectively: the torque to current ratio and internal and connecting wires total resistance. g is the gravity. The dynamics of the driving DC motor-belt system is not represented in the model. The DC motor dynamics can be easily dealt with, at the cost however of increasing the order of the system. The state equations are as follows

$$\begin{aligned}
\dot{x}_1 &= x_3, \\
\dot{x}_2 &= x_4, \\
\dot{x}_3 &= \frac{a_1 w_1(x,u) + w_2(x)\cos x_2}{d(x)}, \\
\dot{x}_4 &= \frac{w_1(x,u)\cos x_2 + a_2 w_2(x)}{d(x)},
\end{aligned} \tag{3}$$

where

$$\begin{aligned}
w_1(x,u) &= k_1 u - x_4^2 \sin x_2 - k_2 x_3 - k_3 \tanh(n x_3), \\
w_2(x) &= g \sin x_2 - k_4 x_4, \\
d(x) &= b - \cos^2 x_2.
\end{aligned}$$

The $a_1, a_2, b, k_1, k_2, k_3$ and k_4 parameters are expressed as follows:

$$a_1 = \frac{J}{m_e l}, \quad a_2 = \frac{1}{l}, \quad b = a_1 a_2 = \frac{J}{m_e l^2}, \tag{4}$$

$$\begin{aligned}
k_1 &= \frac{p_1}{m_e l}, \quad k_2 = \frac{f_c - p_2}{m_e l}, \quad k_3 = \frac{F_s}{m_e l}, \\
k_4 &= \frac{f_p}{m_e l}.
\end{aligned} \tag{5}$$

The control u is constrained

$$|u| \le u_{\max}. \tag{6}$$

3. IDENTIFICATION OF THE MODEL PARAMETERS

The model given above involves six parameters: a_1, a_2, k_1, k_2, k_3 and k_4 to be identified by real-time experiments carried out in the system. In the real system two state variables: x_1 and x_2 are measured with a high accuracy. The former measurement is obtained from 12 bit encoder and the later from similar encoder in a non direct way. The rotational DC motor movement is transferred to the linear cart movement via a belt drive. These encoders are mounted at the pendulum and DC motor shafts. The pendulum angle is measured with the accuracy equal to 0.001534 rad ($2\pi/4096$) and the cart position with the accuracy 0.076 m (one rotation corresponds to the cart shift equal to 0.156 m). The computer sampling period is defined as 0.005 s. The remaining variables x_3 and x_4 are reconstructed (an observer might be introduced). We collect six state trajectories (enumerated by i, $i = 1,\ldots,6$) corresponding to different controls $u^i(k)$ $k = 1,\ldots,N_i$, where k denotes a consecutive point of the trajectory and N_i

is the number of trajectory points in the experiment *i*. These six trajectories are stored in the $\{x_1^i(k), x_2^i(k), x_3^i(k), x_4^i(k)\}$, $k=1,\ldots,N_i$, $i=1,\ldots,6$ concatenated form and become a pattern to be used to fit parameters of the model. The same controls, u^i, $i=1,\ldots,6$ are applied in the model (the initial values of a_1, a_2, k_1, k_2, k_3 and k_4 are guessed). The state trajectories obtained from the model under the control $u^i(k)$ are denoted $\{\tilde{x}_1^i(k), \tilde{x}_2^i(k), \tilde{x}_3^i(k), \tilde{x}_4^i(k)\}$ for $k=1,\ldots,N_i$ $i=1,\ldots,6$. The points of the real (pattern) and model trajectories have to be specified at the same instants. To fit the trajectories an optimization procedure is performed. The multidimensional unconstrained nonlinear minimization Fminsearch (Nelder-Mead) from MATLAB is used with the quality factor Q in the form

$$Q(x,\tilde{x}) = \sum_{i=1}^{6}\sum_{j=1}^{4}\alpha_j \sum_{k=1}^{N_i}\left(x_j^i(k)-\tilde{x}_j^i(k)\right)^2 \qquad \alpha_1=\alpha_3=\alpha_4=1,\ \alpha_2=10 \tag{7}$$

We minimize Q and each Q_i, for $i=1,...,6$, with respect to a_1, a_2, k_1, k_2, k_3 and k_4

$$Q^{\min} = \min_{a_1,a_2,k_1,k_2,k_3,k_4} Q(x,\tilde{x}) \tag{8}$$

$$Q_i^{\min} = \min_{a_1,a_2,k_1,k_2,k_3,k_4} Q_i(x,\tilde{x}),\ i=1,...,6 \tag{9}$$

$Q^{\min}$ is attained at $a_1^\Sigma, a_2^\Sigma, k_1^\Sigma, k_2^\Sigma, k_3^\Sigma, k_4^\Sigma$. This is just the goal of identification to find a unique set common to all real-time trajectories. $Q_i^{\min}$ is attained at $a_1^i, a_2^i, k_1^i, k_2^i, k_3^i, k_4^i$. Obviously $Q^{\min} > \sum_{i=1}^{6} Q_i^{\min}$. For each experiment we calculate

$$\begin{aligned} Q_i^\Sigma &= Q_i(x,\tilde{x},a_1^\Sigma,a_2^\Sigma,k_1^\Sigma,k_2^\Sigma,k_3^\Sigma,k_4^\Sigma) > \\ &> Q_i(x,\tilde{x},a_1^i,a_2^i,k_1^i,k_2^i,k_3^i,k_4^i) = Q_i^{\min}. \end{aligned} \tag{10}$$

The less $Q_i^{\min}$ differs from Q_i^Σ and less $a_1^\Sigma, a_2^\Sigma, k_1^\Sigma, k_2^\Sigma, k_3^\Sigma, k_4^\Sigma$ differ from $a_1^i, a_2^i, k_1^i, k_2^i, k_3^i, k_4^i$ the better is model matching. The switching times and final time for six experiments are shown in Table 1. Table 2 shows the best model matching parameter sets: $a_1^i, a_2^i, k_1^i, k_2^i, k_3^i, k_4^i, Q_i^{\min}$, Q_i^Σ for the experiments. The unique identified parameter set common to all experiments and the minimum $Q^{\min}$ from formula (7) attained for this set are shown in Table 3. To provide an evidence that the attained minimum of quality factor (7) has not got solely a local character the Fminsearch minimization procedure have been repeated 10 times starting from random values of six parameters. The same result as that presented in Table 3 has been obtained. All real-time experiments have been carried out starting from the same initial states $x_0 = \mathrm{col}(0,\ \pi,\ 0,\ 0)$ with different controls $\pm u_{\max}$. Each experimental trajectory consists of 200 points except sixth experiment with 180 points. Each modeled trajectory has approximately five times more points. To have the same number of points an interpolation technique is used. Among five parameters a_1^Σ is perfectly identified. It means that nearly the same values are obtained in each experiment. The parameters of experiment 1 deviate mostly from the average values. In spite of that their values are closest to the unique parameter values commonly evaluated for all experiments.

Table 1. Switching times and the final time

exp. no.	switch 1	switch 2	switch 3	switch 4	switch 5	final
1	0.3	0.8	0.85	1.0	1.76	2.0
2	0.2	0.8	0.95	1.0	1.6	2.0
3	0.5	1.0	1.1	1.2	1.6	2.0
4	0.41	0.82	0.85	1.1	1.7	2.0
5	0.3	0.5	0.8	1.2	1.7	2.0
6	0.41	0.815	0.85	1.05	1.76	1.8

Table 2. The best model matching parameters and corresponding quality factors

exp. no.	a_1^i	a_2^i	k_1^i	k_2^i	k_3^i	k_4^i	$Q_i^{\min}$	Q_i^Σ
1	0.324	64	815	142	77	0.034	19	29
2	0.324	49	583	96	48	0.029	16	25
3	0.326	44	546	77	59	0.025	13	16
4	0.327	43	541	88	48	0.036	19	25
5	0.324	41	502	88	43	0.021	18	23
6	0.325	48	589	73	77	0.015	12	37

Table 3. Identified parameters common to all experiments

a_1^Σ	a_2^Σ	k_1^Σ	k_2^Σ	k_3^Σ	k_4^Σ	$Q^{\min}$
0.3249	62.7	798	112	92.5	0.0356	155

Figs 2 – 5 illustrate six real time experiments (the trajectories are depicted by dotted line). The corresponding modeled trajectories (see formulas (3)) for the identified parameters (see Table 2) are depicted by solid line. In principle the mismatch of the real and modeled trajectories corresponds to the cart position and velocity variables. This is caused by varying cart friction effects. Therefore parameters modeling a given trajectory do not need to fit perfectly to model another

trajectory. Nevertheless the model error is acceptable, as we can see further, to extract the time optimal control to be used even in the open loop. There is the small velocity zone depicted in Fig. 4.

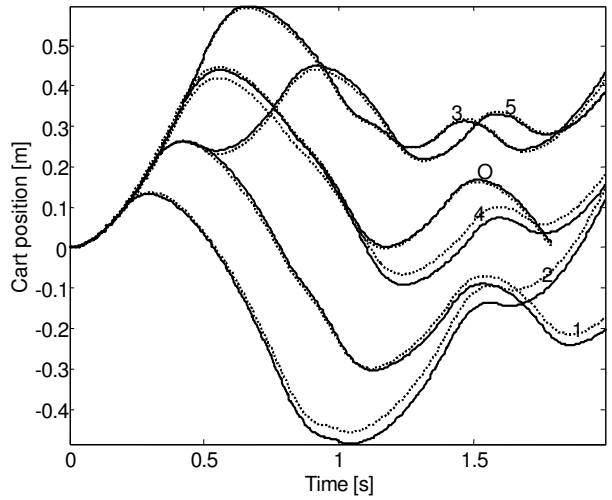

Fig. 2. Cart positions in six experiments; real measured – dot line; commonly modeled – solid line

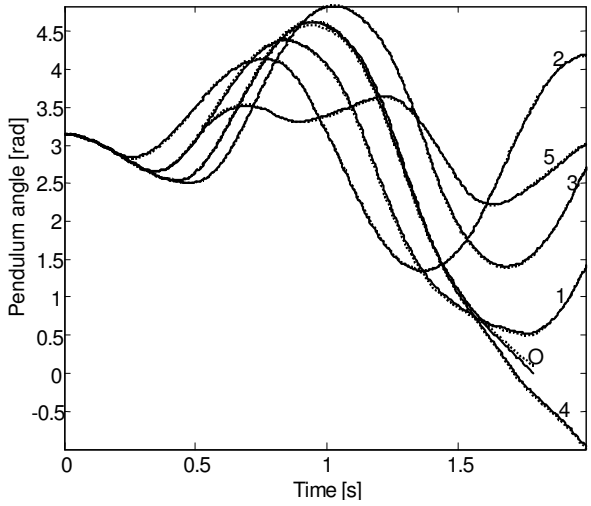

Fig. 3. Pendulum angles in six experiments; real measured – dot line; commonly modeled – solid line

The trajectory points that belong to this zone are excluded from the $Q(x,\tilde{x})$ set in formula (7). In this way we avoid large errors related to the reconstructed (calculated not measured) velocities x_3 and x_4. This is the crucial idea to obtain a more accurate parameter fitting. One can notice that the excluded points lead to the identification procedure performed in intervals. The first and second intervals of trajectory No. 2 are depicted in Fig. 4. Having identified five model parameters we can extract the physical parameters of the system. From formula (4) $l = 1/a_2 = 0.01595$ m, $J/m_e = a_1 l = 0.005182$ m^2 and b = 20.37123. The total mass of the system, m can be measured with a high accuracy. However we need to use the equivalent mass m_e. Thus it seems to be better to calculate the pendulum inertia momentum J on the basis of the pendulum geometrical shape. Using the well known formulas of mechanics we obtain J = 0.00527 kgm^2. Hence, m_e = 1.017 kg (the weighted mass, m = 0.56 kg). From formula (2) $p_1 = k_1 m_e l$, p_1 = 12.9439 N, $\varepsilon = p_1 / K_u$ and taking K_u = 24 V we calculate ε = 0.5393 NV^{-1}. After calculating ε we can extract the internal motor and connecting wires resistance $R_i = M_i/(\varepsilon r_d)$. The torque to current ratio M_i = 0.0477 NmA^{-1} is a catalogue nominal parameter of the motor.

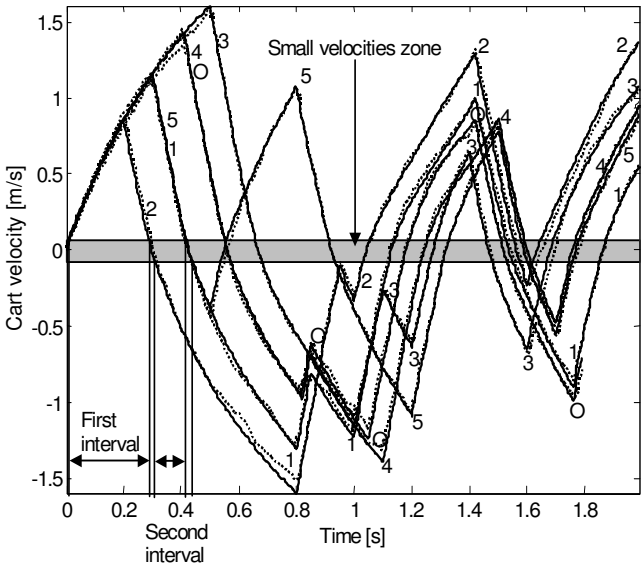

Fig. 4. Cart velocity in six experiments; real observed – dot line; commonly modeled – solid line

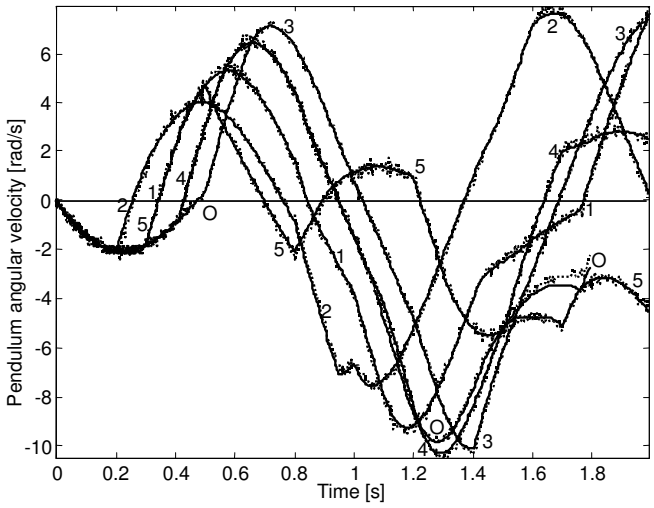

Fig. 5. Pendulum velocity in six experiments; real observed – dot line; commonly modeled – solid line

The wheel radius r_d = 0.0341 m is measured. Hence, we obtain R_i = 2.594 Ω. On the basis of the other catalogue nominal value, U_{rpm} = 5 mV(rpm)$^{-1}$ and from formula (2)

$p_2 = -\ 0.75516$ Ns/m. Finally, from formula (5) we have $f_c = k_2 m_e l + p_2$, $F_s = k_3 m_e l$ and $f_p = k_4 m_e l$. Their values are as follows: $f_c = 1.0615$ Ns(m)$^{-1}$, $F_s = 1.5004$ N and $f_p = 5.7745 \cdot 10^{-4}$ Nms(rad)$^{-1}$.

4. TIME-OPTIMAL CONTROL

The identified model has to be verified in real-time. Fig. 6 and Fig. 7 present results of ten repeated experiments.

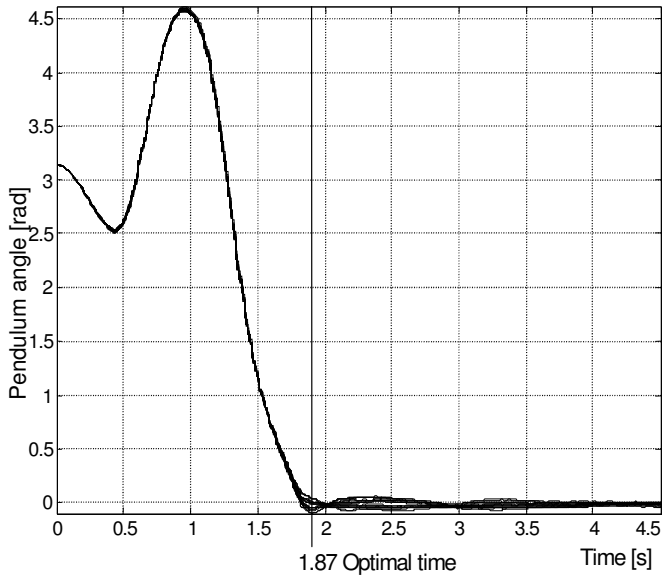

Fig. 6. Pendulum angles in ten real-time experiments

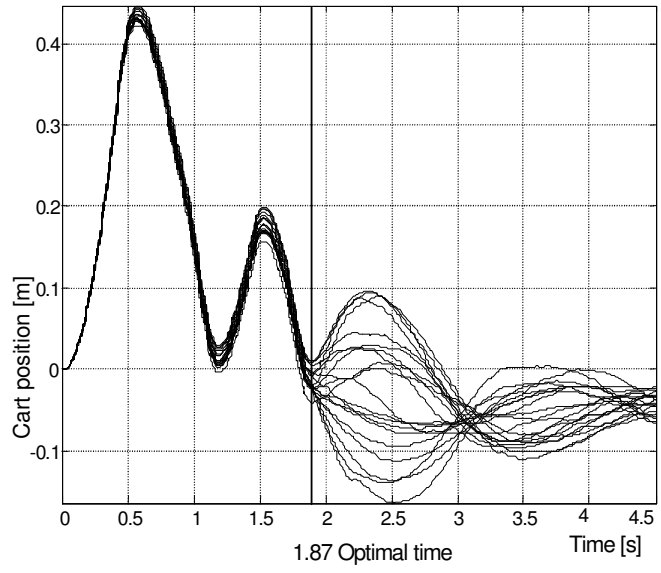

Fig. 7. Cart positions in ten real-time experiments

Consider the optimization problem x_0 = col(0, π, 0, 0) and open-loop unstable target state x^f = 0. The numerical algorithm is applied to the pendulum on a cart model with parameters: $a_1^\Sigma, a_2^\Sigma, k_1^\Sigma, k_2^\Sigma, k_3^\Sigma, k_4^\Sigma$ (see Table 3) and admissible control u (see formula (6)) with $u_{\max} = 0.5$. The most critical model utility test is the open loop time-optimal control. To perform such a test we use here the optimization procedures described in (Turnau, *et al.*, 1999) and evaluated in (Turnau, *et al.*, 2005). The method has been developed further. The approach proposed below is applied also to varying control structure. This is achieved by combining the linearized feedback scheme with the *monotonous structure evolution* (Szymkat, *et al.*, 2003). The new method gives good disturbance rejection at a low computational cost. The conjugate equations corresponding to the state equations (3 – 5) and the control constraints (6) have the following form

$$\begin{aligned}
\dot{\psi}_1 &= 0, \\
\dot{\psi}_2 &= A_{23}(x,u)\psi_3 + A_{24}(x,u)\psi_4, \\
\dot{\psi}_3 &= -\psi_1 + A_{33}(x)\psi_3 + A_{34}(x)\psi_4, \\
\dot{\psi}_4 &= -\psi_2 + A_{43}(x)\psi_3 + A_{44}(x)\psi_4.
\end{aligned} \tag{11}$$

where:

$$\begin{aligned}
A_{23} &= \frac{x_4^2 \cos x_2 - \cos^2 x_2 + V_2 \sin x_2 + F_3 \sin 2x_2}{D}, \\
A_{24} &= \frac{x_4^2 \cos^2 x_2 - b \cos x_2 + V_1 \sin x_2 + F_4 \sin 2x_2}{D}, \\
A_{33} &= \frac{1}{D}\left(c_1 + \frac{n\alpha_3 u_s}{\cosh^2 (n\alpha_3 x_2)} \right), \\
A_{43} &= \frac{2x_4 \sin x_2 + c_2 \cos x_2}{D}, \\
A_{44}(X) &= \frac{X_4 \sin 2X_2 + c_2 b}{D(X)}.
\end{aligned} \tag{12}$$

The gradient has the form

$$g = -\frac{\psi_3 + \psi_4 \cos X_2}{D}. \tag{13}$$

If singularities do not occur the time optimal control has the bang-bang character

$$u(t) = \begin{cases} u_{\max}, & \text{if} \quad \psi_3(t) + \psi_4(t)\cos x_2(t) > 0 \\ -u_{\max}, & \text{if} \quad \psi_3(t) + \psi_4(t)\cos x_2(t) < 0 \end{cases}. \tag{14}$$

The following sequence of "bang-bang" control time switchings (in seconds) is obtained: 0.4016 0.775 0.826 1.0575 1.411 1.748 and the final control time, 1.859. These values are rounded off to 5 ms that is the sampling period value in the real system: 0.40 0.78 0.83 1.06 1.41 1.75 and 1.86. Next, two sampling periods are added to each switching time. Because the real system when starts remains two sampling periods delayed. Finally, the time switchings in (see Table 4) up to the horizon are applied in the real-time open loop control experiments. They prove reliably sufficient accuracy of the identified model. If the identified model were not accurate one would never be able to achieve the control target successfully and repeatedly in the open loop.

Table 4. Time switchings in the real-time experiments

sw. 1	sw. 2	sw. 3	sw. 4	sw. 5	sw. 6	horizon
0.41s	0.79s	0.84s	1.0s	1.42 s	1.76s	1.87s

Two trajectory bundles in Figs 6 and 7 related to the pendulum angular position and the cart position are sufficiently narrow – from the control beginning to its horizon – to believe to a good quality of the model. Notice, this observation is valid till 1.87 s at both figures. Later, in some predetermined neighborhood of the target (when a small vicinity of the pendulum upright equilibrium point is achieved ($|x_2| \le 0.08$ [rad]) the time-optimal open-loop control is replaced by a stabilizing controller. In our experiments an l-q optimal controller is used keeping the pendulum in the upright position simultaneously centering the cart in the middle of the rail (see Fig. 7). Therefore, to verify correctness of the identified parameters we refer only to the parts of Fig. 6 and Fig. 7 limited by the horizon vertical line at 1.87 s. Later points of the trajectory bundles are not used to identify the model. There are two effects related to discrete nature of measurement and control signals: the computer sampling period equal to 0.005 s and the quantization determined by the construction of sensing devices – the encoders. Further diminishing the sampling period is not recommended. First, it must be a trade-off between quantization and sampling. Second, for a closed-loop time-optimal control we do require time to repeat an optimization procedure.

5. CONCLUSIONS

The model construction and parameter identification procedures are complex tasks. If a control goal is defined it helps to diminish a set of system trajectories to be involved into the model fitting. This is the most important issue of the proposed identification method. The model identification becomes dedicated to the time-optimal control. The parameter identification procedure is narrowed only to "bang-bang" trajectories. Moreover, motionless or slow velocities trajectory points are excluded. In this way disturbances generated by static friction effects are neglected. The identification processed in intervals yields the more accurate modeling

ACKNOWLEDGMENTS

The author would like to thank the anonymous reviewer for valuable remarks.

The research work is supported by the Ministry of Science and Higher Education as a part of the research program No. KBN 4 T07C 01630.

REFERENCES

Eykhoff, P. (1974). *Identification. Parameter and State Estimation*. John Wiley and Sons, London.

Gershenfeld, N. (1999). *The Nature of Mathematical Modeling*. Cambridge University Press, UK.

Marchewka D. and A. Turnau (2005). Identification of 3DOF manipulator oriented to time-optimal control. CMS'05, *Computer Methods and Systems*, Kraków, pp. 125-128.

Szymkat, M. and A. Korytowski (2003). Method of monotone structural evolution for control and state constrained optimal control problems. *European Control Conference*, University of Cambridge, UK, 6 p.

Turnau A., A. Korytowski and M. Szymkat (1999). Time optimal control for the pendulum cart system in real-time. *Proceedings IEEE of International Conference on Control Applications*, Kohala Coast-Island of Hawai'i, USA, pp. 1249-1254.

Turnau A., M. Szymkat, A. Korytowski and K. Kołek (2005). A robust repetitive scheme with relaxed minimum time criterion. *16 IFAC World Congress*, Prague, 6 p.